

# Influence of Microwave Heating on the Growth of Gadolinium-Doped Cerium Oxide Nanorods

Mario Godinho,<sup>†</sup> Caue Ribeiro,<sup>‡</sup> Elson Longo,<sup>†</sup> and Edson Roberto Leite<sup>\*,†</sup>

Chemistry Department, Federal University of São Carlos, CP-676, 13565-905, São Carlos, SP, Brazil, and EMBRAPA Instrumentação Agropecuária, CP- 741, 13569-970, São Carlos, SP, Brazil

Received September 11, 2007; Revised Manuscript Received October 19, 2007

**ABSTRACT:** In this communication, we demonstrate that the use of microwave heating during hydrothermal treatment drastically decreases the treatment time required to obtain gadolinium-doped ceria nanorods and that the oriented attachment is the dominant mechanism responsible for anisotropic growth. In fact, considering oriented attachment (OA) as a statistical mechanism, we postulate that the growth process conducted under microwave heating increases the effective collision rate. A plausible explanation for the increase of the effective collision rate under microwave irradiation is the increase in the collision cross-section of the particle.

Cerium oxide (ceria) and doped cerium oxide (doped ceria) are rare earth oxides that have been extensively studied and applied in catalysis, electrochemistry, UV blockers, and polishing materials.<sup>1</sup> In recent years, ceria and doped ceria anisotropic nanocrystals, mainly nanorods, have been obtained through several solution-based synthetic routes<sup>2</sup> with special attention focusing on routes based on the precipitation and aging of the precipitate under hydrothermal conditions.<sup>2a,b,3</sup> The main reason for this interest in ceria-based anisotropic nanocrystals is the possibility of developing catalytic materials with a high surface area and well-defined reactive crystal planes with superior catalytic activity.<sup>3</sup> However, to control the size and shape of nanocrystals during their synthesis, it is fundamental to understand the predominant growth mechanism. Despite the progress reported for the synthesis of ceria nanorods, the mechanism responsible for the growth process remains unclear. For instance, Kuiry et al.<sup>2d</sup> reported the synthesis of ceria polycrystalline nanorods and proposed a growth mechanism based on the preferential assembly of ceria nanocrystallites in a longitudinal direction (they proposed a mechanism that was not based on a nucleation and growth process). Mai et al.<sup>2b</sup> described the synthesis of single crystal ceria nanorods and attributed the growth mechanism to a nucleation and growth process controlled mainly by dissolution/recrystallization in hydrothermal conditions at a high pH (pH > 10) and a temperature of around 100 °C. However, very recently the oriented attachment (OA) mechanism was observed as a predominant growth process of self-organized ceria nanocrystals and in nanorods.<sup>4</sup>

A more in-depth analysis of the growth mechanism, such as OA, can shed light on the formation of these anisotropic nanostructures. The number of materials obtained by the OA process is growing rapidly<sup>5</sup> and has become an attractive form of processing nanomaterials with anisotropic structure. The OA mechanism originally proposed by Banfield and Penn<sup>6</sup> is a process involving the self-organization of adjacent nanocrystals and coalescence. This mechanism is related to the collision rate among the nanocrystals in suspension and to the reduction of surface energy, aimed at minimizing the area of high-energy faces.<sup>7</sup>

In the present report, we show that the anisotropic nanocrystalline morphology of gadolinium-doped ceria oxide is related to the OA nanocrystal growth mechanism and that microwave heating influences the growth process. To this end, we use a process based on precipitation at room temperature and aging of the precipitate under hydrothermal conditions in a traditional oven and in a microwave oven.

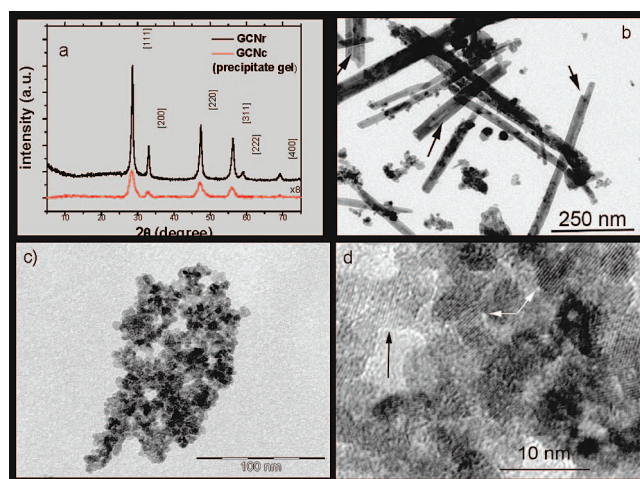


**Figure 1.** (a) XRD pattern of the material before and after hydrothermal treatment in MwO; (b) BF-TEM image of the material after hydrothermal treatment in MwO; (c) BF-TEM image of the material after hydrothermal treatment in EO; (d) HRTEM image of the material after hydrothermal treatment in EO (the arrows indicate coalescence events typical of the AO mechanism).

Following a typical procedure for the synthesis of gadolinium-doped ceria nanocrystals (GCNc), 0.1 mol/L of hexahydrated cerium(III) nitrate ( $\text{Ce}(\text{NO}_3)_3 \cdot 6\text{H}_2\text{O}$ , 99.9%, Aldrich, USA) was dissolved in high purity water in polytetrafluoroethylene (PTFE) vessels. After complete dissolution of the cerium nitrate, gadolinium(III) oxide ( $\text{Gd}_2\text{O}_3$ , 99.9%, Aldrich, USA) dissolved in a minimal amount of nitric acid was then added to the solution to obtain a nominal composition of  $\text{Gd}_{0.2}\text{Ce}_{0.8}\text{O}_{2-x}$ . Under magnetic stirring, ammonium hydroxide (0.1 mol/L) was added dropwise to complete the precipitation (final pH = 10), resulting in a white gel. It is important to point out that X-ray diffraction (XRD) analysis of the dry gel (dried at room temperature for 48 h) indicated the formation of a single phase of GCNc with a cubic fluorite structure (see Figure 1a). The PTFE vessels containing the GCNc in water suspension were then treated under a hydrothermal condition (130 °C, 3 atm pressure, for 30 min). The hydrothermal treatment was carried out in a traditional electric oven (EO) or in a microwave oven (MwO). After the hydrothermal treatment, the powder in suspension was centrifuged and washed in distilled water until the residual ions in the solution were completely eliminated. The resulting product was dried at room temperature for 48 h and characterized by transmission electron microscopy (TEM), high-resolution transmission electron microscopy (HRTEM, Philips CM 200 operated at 200

\* To whom correspondence should be addressed. E-mail: derl@power.ufscar.br.

<sup>†</sup> Federal University of São Carlos.

<sup>‡</sup> EMBRAPA Instrumentação Agropecuária.

kV), and X-ray diffraction (XRD) (Rigaku D-Max 2500, using Cu K $\alpha$  radiation).

The gadolinium-doped ceria nanorods (GCNr), with a nominal composition of Gd<sub>0.2</sub>Ce<sub>0.8</sub>O<sub>2-x</sub>, were synthesized by hydrothermal treatment of a colloidal suspension of GCNc in an aqueous solution. XRD and TEM analysis of the synthesized material presented interesting results in terms of its crystallographic phase and morphology. Figure 1a shows the XRD pattern of the material before and after hydrothermal treatment in a microwave oven (MwO). Before the treatment, one can observe a pattern of a crystalline material (single phase with cubic fluorite structure) composed of broad peaks typical of nanocrystalline materials. The crystallite size, calculated from XRD data and Scherrer's equation, was 3.1 nm. TEM and HRTEM characterization of the as-precipitated material shows the presence of well-crystallized nanoparticles with a spherical morphology and sizes ranging from 3 to 5 nm.<sup>8</sup> After the hydrothermal treatment, the material preserved the fluorite structure with a well-defined XRD pattern (narrow peaks), suggesting that no phase transformation occurred during the treatment. The better definition of the XRD pattern is probably ascribable to the growth process. Figure 1b shows the bright field (BF) TEM image of the material after hydrothermal treatment in MwO, indicating the presence of GCNr and GCNc. The GCNr presented a length ranging from 50 to 500 nm and a diameter of 20–60 nm. The synthesized GCNr displayed a morphology similar to that reported by Zhou et al.<sup>3</sup> and Mai et al.,<sup>2b</sup> however, those studies used traditional heating and longer treatment times (>24 h). In the present work, the use of microwave heating allowed for a shorter treatment time (30 min). A control experiment performed under hydrothermal conditions, using traditional heating (EO) and similar experimental parameters (temperature, time, composition, and pressure) did not show the formation of GCNr. The only formation observed was GCNc with a particle size ranging from 10 to 15 nm (see TEM and HRTEM images in Figure 1c,d). This result clearly indicates that microwave heating accelerates the formation of nanorods. TEM coupled with energy dispersive spectroscopy study (not shown here) and XRD analysis of the nanostructured material before and after hydrothermal treatment confirmed that Gd was in solid solution in the ceria lattice.

A closer examination of the BF-TEM image in Figure 1b reveals that the GCNr is composed of several nanoparticles, as indicated by the arrows. This finding offers important information and can shed light on the crystal growth mechanism. The HRTEM characterization of the material after hydrothermal treatment presented interesting results concerning the GCNr formation mechanism. The HRTEM images in Figure 2a–c confirm that the anisotropic particles were composed of several primary particles. In fact, the HRTEM image reveals that the nanorods were composed of oriented primary particles, as indicated by the arrows in Figure 2a and by the additional images in Figure 2b,c. Figure 2b,c depicts reconstructed lattice images of different areas (as indicated in Figure 2a), showing boundaries between particles (indicated by the dashed white line in Figure 2b) and a region with perfect attachment and alignment between particles, without defects (Figure 2c). Figure 3a–c shows interesting HRTEM images of a nanorod with a imperfect attachment. The imperfectly oriented attachment may produce different kinds of defects, depending on the rotational relation of one nanocrystal to the other.<sup>6</sup> Figure 3b,c (reconstructed lattice images) shows details of the imperfect alignment.

The aggregation of several nanocrystals with similar crystallographic orientations originating a single nanorod, as well as the presence of defects, is strong evidence that the OA process is the predominant nanocrystal growth mechanism<sup>5–7</sup> during the processing of GCNr. The HRTEM results (Figure 3a) revealed that the diameter dimensions of the nanorod were related to the (002) direction of the lattice. We also observed the lattice direction (111). This crystallographic information indicates the formation of nanorods with preferential growth in the [110]. This growth direction is in agreement with the fact that the driving force for the

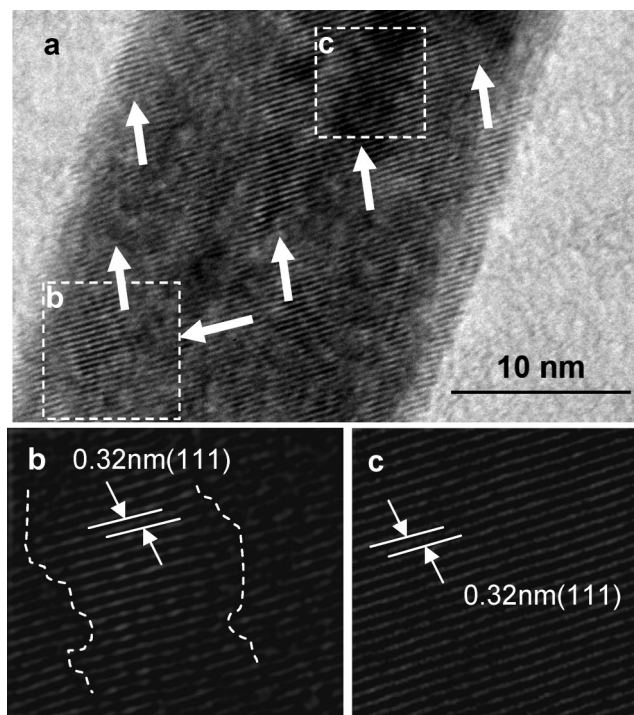


**Figure 2.** (a) HRTEM image of the material after hydrothermal treatment in MwO; (b, c) reconstructed lattice images of different areas (indicated in panel a).

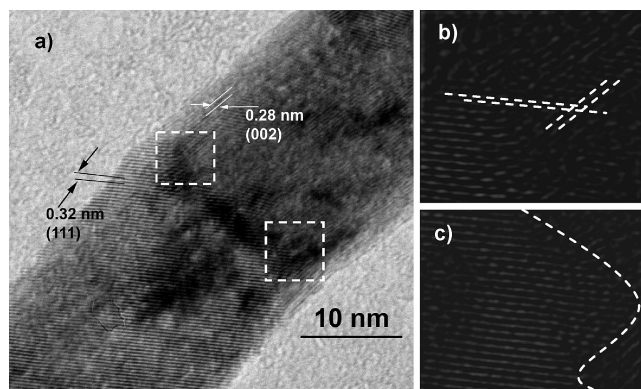


**Figure 3.** (a) HRTEM image of the material after hydrothermal treatment in MwO; (b, c) reconstructed lattice images of different areas (indicated in panel a).

coalescence process in the OA mechanism is related to the reduction of surface energy, aimed at minimizing the area of high-energy faces. In a cubic system, the {111} plane is the more stable one (presenting the lowest surface energy). Thus, growth in {110} is expected.

It is important to note that no remarkable preferential growth is observed in the XRD pattern of the GCNr sample (Figure 1a). This is surprising, because one would expect that the preferential growth in the [110] direction, as observed by HRTEM (Figures 2 and 3), should lead to an increase of the (220) reflection. However, a close look at the TEM and HRTEM images (Figures 1b, 2a, and 3a) shows a simultaneous growth process along the [200] and [111] directions, and not only in the [110] direction. Thus, an increase in intensity of the (200) and (111) reflections should occur, resulting in a XRD pattern with no evidence of preferential growth. Besides, the XRD analysis was performed in a sample without purification, that is, in a sample with nanorods and nanocrystals. The presence of nanocrystal can modify the intensity of the reflections, especially the (111) reflection.



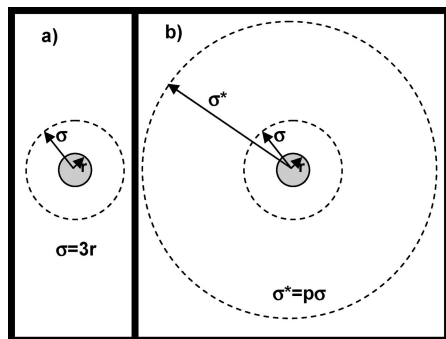


**Figure 4.** Schematic representation of (a) noninteractive cross-section, and (b) interactive cross-section.

From the kinetic standpoint, the OA mechanism can be divided in two steps: (a) particles collisions and (b) coalescence.<sup>7a,9,10</sup> An interesting finding provided by our experimental data is the fact that, under microwave heating, the growth process of GCN<sub>r</sub> is faster than under normal electric heating. It should be noted that nanoparticle coalescence took place in both processes (with and without microwave heating). Figure 1d provides strong evidence of the OA mechanism in the material's growth in the hydrothermal condition under traditional heating. The observation of nanoparticle coalescence in both hydrothermal treatments (with and without microwave heating) suggests that the coalescence process is not the lowest step in the OA mechanism. We therefore postulate that collision is the rate-determining step and that it controls the kinetics of this mechanism. On the basis of this assumption, we can suggest that microwave heating increases the collision rate, resulting in faster nanorod growth. In fact, considering the OA as a statistical mechanism,<sup>9</sup> we can postulate that the growth process conducted under microwave heating increases the effective collision rate. Effective collision occurs when particles collide, producing an irreversibly oriented attachment, and this occurs only if their orientations at the time of collision achieve a congruent two-dimensional structure at the interface.<sup>9,10</sup>

A plausible explanation for the increase of the effective collision rate under microwave irradiation is the increase in the collision cross-section ( $\sigma$ ) of the particle. In a previous article,<sup>9</sup> we made a detailed kinetic analysis of the OA mechanism, in which we assumed the occurrence of a noninteractive collision with a  $\sigma = 3r$ , where  $r$  is the particle's radius. Under microwave irradiation, we can suppose an interactive collision introducing a steric factor ( $P$ ), and expressing the interactive cross-section ( $\sigma^*$ ) as a multiple of  $\sigma$

$$\sigma^* = P\sigma \quad (1)$$

where  $P > 1$ . A schematic representation of a noninteractive and interactive cross-section is illustrated in Figure 4. The origin of the interactive collision and, hence, of the steric factor, should be the instantaneous dipole moment generated in the nanocrystal by the electromagnetic field induced by microwave radiation. Actually, the instantaneous dipole will generate dispersive force between the nanocrystals, and this kind of attractive force is related to the steric factor.

From the experimental results presented here, it is not possible to separate the rate enhancement caused by the rapid and uniform

heating from the intrinsic effects of microwave radiation, such as interactive collision. However, the effect of microwave heating on the growth process is clear, and the hypothesis presented here serves as a starting point to introduce dispersive force as a kinetic parameter in the OA mechanism. It is well accepted that the OA mechanism can be controlled by the addition of surfactants and passivating molecules or by changing the solvent.<sup>7b,10,11</sup> On basis of the results presented here and in recent publications on the microwave-assisted synthesis of anisotropic ZnO<sup>12a</sup> and iron oxide<sup>12b</sup> nanocrystals, we can speculate that the use of microwave heating can serve as an alternative way to improve control over the OA mechanism.

In summary, we demonstrated that the use of MwO during hydrothermal treatment drastically decreases the treatment time required to obtain GCN<sub>r</sub> and that the OA is the dominant mechanism responsible for anisotropic growth.

**Acknowledgment.** Financial support by FAPESP and CNPq (both Brazilian agencies) is gratefully acknowledged.

## References

- (1) (a) Namai, Y.; Fukui, K. I.; Iwasawa, Y. *J. Phys. Chem. B* **2003**, *107*, 11666–11673. (b) Minh, N. Q. *J. Am. Ceram. Soc.* **1993**, *73*, 563–568. (c) Wang, Z.; Feng, X. *J. Phys. Chem. B* **2003**, *107*, 13563–13566. (d) Feng, X.; Sayle, D. C.; Wang, Z. L.; Paras, M. S.; Santora, B.; Sutorik, A. C.; Sayle, T. X. T.; Yang, Y.; Ding, Y.; Wand, X.; Her, Y.-S. *Science* **2006**, *312*, 1504–1508.
- (2) (a) Han, W.-Q.; Wu, L.; Zhu, Y. *J. Am. Chem. Soc.* **2005**, *127*, 12814–12815. (b) Mai, H.-X.; Sun, L.-D.; Zhang, Y.-W.; Si, R.; Feng, W.; Zhang, H.-P.; Liu, H.-C.; Yan, C.-H. *J. Phys. Chem. B* **2005**, *109*, 24380–24385. (c) Zhang, D.; Fu, H.; Shi, L.; Pan, C.; Li, Q.; Chu, Y.; Yu, W. *Inorg. Chem.* **2007**, *46*, 2446–2451. (d) Kuiry, S. C.; Patil, S. D.; Deshpande, S.; Seal, S. *J. Phys. Chem. B* **2005**, *109*, 6936–6939. (e) Lee, J. S.; Kim, S. *J. Am. Ceram. Soc.* **2007**, *90*, 661–663.
- (3) Zhou, K.; Wang, X.; Sun, X.; Peng, Q.; Li, Y. *J. Catal.* **2005**, *229*, 206–212.
- (4) (a) Si, R.; Zhang, Y.-W.; You, L.-P.; Yan, C.-H. *J. Phys. Chem. B* **2006**, *110*, 5994–6000. (b) Du, N.; Zhang, H.; Chen, B.; Ma, X.; Yang, D. *J. Phys. Chem. C* **2007**, *111*, 12877–12680.
- (5) (a) Coelfen, H.; Antonietti, M. *Angew. Chem., Int. Ed.* **2005**, *44*, 5576–5591. (b) Niederberger, M.; Colfen, H. *Phys. Chem. Chem. Phys.* **2006**, *8*, 3271–3287.
- (6) (a) Penn, R. L.; Banfield, J. F. *Am. Mineral.* **1998**, *83*, 1077–1082. (b) Penn, R. L.; Banfield, J. F. *Science* **1998**, *281*, 969–971. (c) Penn, R. L.; Banfield, J. F. *Geochim. Cosmochim. Acta* **1999**, *63*, 1549–1557.
- (7) (a) Leite, E. R.; Giraldo, T. R.; Pontes, F. M.; Longo, E.; Beltran, A.; Andres, J. *Appl. Phys. Lett.* **2003**, *83*, 1566–1568. (b) Polleux, J.; Pinna, N.; Antonietti, M.; Hess, C.; Wild, U.; Schlögl, R.; Niederberger, M. *Chem. Eur. J.* **2005**, *11*, 3541–3551.
- (8) Godinho, M. J.; Goncalves, R. F.; Santos, L. P. S.; Varela, J. A.; Longo, E.; Leite, E. R. *Mater. Lett.* **2007**, *61*, 1904–1907.
- (9) Ribeiro, C.; Lee, E. J. H.; Longo, E.; Leite, E. R. *ChemPhysChem* **2005**, *6*, 690–696.
- (10) Penn, R. L. *J. Phys. Chem. B* **2004**, *108*, 12707–12712.
- (11) Cho, K. S.; Talapin, D. V.; Gaschler, W.; Murray, C. B. *J. Am. Chem. Soc.* **2005**, *127*, 7140–7147.
- (12) (a) Hu, X.-L.; Zhu, Y.-J.; Wang, S.-W. *Mater. Chem. Phys.* **2004**, *88*, 421–426. (b) Wang, W.-W.; Zhu, Y.-J.; Ruan, M.-L. *J. Nanoparticle Res.* **2007**, *9*, 419–426.

CG700872B